Physical Modeling of Nonlinear Player-String Interactions in Bowed String Sound Synthesis Using Finite Difference Methods

C. Desvages[a] and S. Bilbao[b]
[a]University of Edinburgh, Room 1608, JCMB, Kings Buildings, Mayfield Rd., EH9 3JZ Edinburgh, UK
[b]University of Edinburgh, Room 1602, JCMB, Kings Buildings, Mayfield Rd., EH9 3JZ Edinburgh, UK
s1260130@sms.ed.ac.uk

Sound synthesis for continuously excited musical instruments via physical modelling requires, for realism, a time varying input, simulating the player's gesture. A two-polarisation physical model of a bowed string is designed, with bow-string and finger-string nonlinear interactions. The Hunt and Crossley damped collision model is used for contact interactions in a plane orthogonal to the bow, and a "friction curve" model describes the relative velocity dependent friction forces in a plane parallel to the bow. A finite difference scheme is implemented for this model, allowing for numerical simulation of the full system. Sound examples are given to illustrate the range of bowed string gestures that can be artificially reproduced with such a model.

1 Introduction

Sound synthesis for stringed instruments has employed physical modeling techniques for almost half a century; however, in recent years, there has been a tendency towards increased detail in the models of the underlying processes, leading, ultimately, to great increases in the quality of synthetic sound output.

The first attempts at string simulation relied on discretising and numerically solving the wave equation [1, 2], but were somewhat restricted by the limited power of digital computers at the time. Later models such as the Karplus-Strong algorithm [3] and the more recent and still widely used digital waveguide formalism, introduced by Smith in 1985 [4], have produced convincing sound outputs, while staying computationally efficient enough to allow real-time synthesis, as reported in [5]. A digital waveguide simulation of a string relies on modelling forward and backward travelling waves; it is indeed efficient for linear time invariant systems, as losses and dispersion can be lumped at one point.

However, a real string interacts with its environment in a complex manner. The model proposed here comprises two polarisations for the transverse motion of the string, and accounts for three external "objects": the bow (more specifically, the bow hair), the player's finger, and the neck of the instrument. Their action on the string is covered by a nonlinear collision model in the vertical polarisation (that is, in a plane orthogonal to the bowing direction), and a nonlinear friction curve model in the horizontal polarisation (in a plane parallel to the bow).

Such a model can be simulated with standard digital waveguide or modal synthesis techniques with difficulty (see [6] for an example); the string is subjected to the action of distributed collision and friction forces. Finite difference methods [7], while requiring significantly more computational power, can be used to numerically solve a system of partial differential equations, while making minimal assumptions on the form of the solution. This framework simplifies design in the present setting, where multiple nonlinear interactions are modelled.

Bowed string instruments rely on a continuous excitation mechanism, unlike struck or plucked string instruments, and hence the player's input is of prime importance throughout the duration of a note. The playability of virtual instruments has been extensively investigated by various authors [8, 9, 10]; bowing gestures can be described by only a few dynamic parameters. Askenfelt [11, 12] describes a setup for measuring bow force, velocity, and bow-bridge distance in typical gestures. More recent attempts at measuring these parameters for analysis and resynthesis have been achieved by Demoucron [13] and Maestre [14, 15], in order to map bowing patterns to mathematical functions to be fed into a numerical model. A computational physical model such as the one presented in this paper allows for full dynamic control over these excitation parameters, hence subtle and realistic sound synthesis can be achieved.

Section 2 introduces the physical model for a bowed string, including a description of the nonlinear interactions at work in both polarisations, namely the contact interaction and the tangential friction. Section 3 demonstrates synthesis of sounds through a finite difference implementation of the physical model, under realistic gesture parameters reproduction.

2 A two-polarisation string model

2.1 String properties and equations of motion

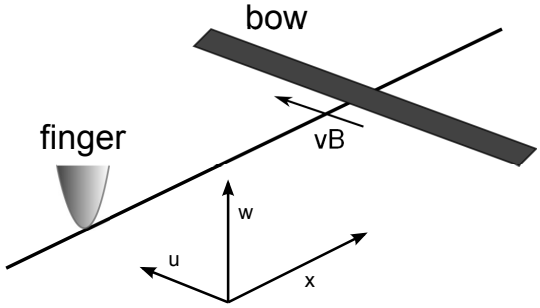

Figure 1: *Choice of coordinates for the model. u and w are the dependent variables for the horizontal and vertical displacement of the string, respectively. x is the space coordinate along the string.*

The model consists of a linear stiff string, with frequency dependent losses, and simply supported boundary conditions; the choice of coordinates is shown in figure 1. The equations of motion for the variables $w(x,t)$ and $u(x,t)$ representing the displacement of the string in the vertical and horizontal directions at position $x \in \mathcal{S} = [0, L]$ and time $t \in \mathbb{R}^+$ can now be written as:

$$\rho \frac{\partial^2 w}{\partial t^2} = T \frac{\partial^2 w}{\partial x^2} - B \frac{\partial^4 w}{\partial x^4} - \lambda_1 \rho \frac{\partial w}{\partial t} + \lambda_2 \rho \frac{\partial^3 w}{\partial t \partial x^2} + \mathcal{F}_N - J_F f_F - J_B f_B \tag{1a}$$

$$\rho \frac{\partial^2 u}{\partial t^2} = T \frac{\partial^2 u}{\partial x^2} - B \frac{\partial^4 u}{\partial x^4} - \lambda_1 \rho \frac{\partial u}{\partial t} + \lambda_2 \rho \frac{\partial^3 u}{\partial t \partial x^2} - (\mathcal{F}_N)_+ \varphi_N - J_F (f_F)_+ \varphi_F - J_B (f_B)_+ \varphi_B \tag{1b}$$

where $(\cdot)_+$ is equivalent to $\max(\cdot, 0)$. As the various surfaces in contact are not considered adhesive, friction only occurs when $f_F(t)$ and $f_B(t)$ are positive. The string has a linear mass density ρ in kg/m, a tension T in N. B is its bending stiffness, defined by $B = EI_0$ where E is Young's modulus of the string

material in Pa and I_0 is the area moment of inertia (for a cylindrical string, $I_0 = \frac{\pi}{4} r^4$, with r the radius of the string in m). λ_1 and λ_2 are positive coefficients accounting respectively for the frequency independent and dependent energy losses intrinsic to the string.

$\mathcal{F}_N(x,t)$ is the contact force density exerted by the neck on the string along its length, in N/m. $f_F(t)$ and $f_B(t)$ are the contact forces respectively exerted by the finger and bow on the string; they act over two time-varying spatial distributions $J_F(x,t)$ and $J_B(x,t)$, normalised over the length of the string. For simplicity, this model makes use of Dirac delta functions, such that the bow and finger act on one point of the string. The contact forces will be explicitly defined in section 2.2, along with the friction curves φ_N, φ_F and φ_B.

2.2 Contact interactions in the vertical polarisation

2.2.1 Contact forces for the finger and bow

The contact forces for the finger and the bow can be written as a function of a derived potential $\Phi(t)$, summed with a damping term as a function of $\Psi(t)$, allowing strict energy dissipation, as later demonstrated (see section 2.2.3).

$$f_F = \frac{\dot{\Phi}_F}{\dot{\Delta}_F} + \dot{\Delta}_F \Psi_F \qquad f_B = \frac{\dot{\Phi}_B}{\dot{\Delta}_B} + \dot{\Delta}_B \Psi_B \tag{2}$$

The variables $\Delta_F(t)$ and $\Delta_B(t)$ can be interpreted as a *deformation* if the colliding object is soft, or a *penetration*, if the collision is rigid.

$$\Delta_F = \int_S J_F w \, dx - w_F \qquad \Delta_B = \int_S J_B w \, dx - w_B \tag{3}$$

$w_F(t)$ and $w_B(t)$ are respectively the position of the finger and bow above the string. A choice of expression for the potential and damping function comes as:

$$\Phi_F = \frac{K_F}{\alpha_F + 1} (\Delta_F)_+^{\alpha_F + 1} \qquad \Psi_F = K_F \beta_F (\Delta_F)_+^{\alpha_F} \tag{4a}$$

$$\Phi_B = \frac{K_B}{\alpha_B + 1} (\Delta_B)_+^{\alpha_B + 1} \qquad \Psi_B = K_B \beta_B (\Delta_B)_+^{\alpha_B} \tag{4b}$$

with $K_F, K_B \geqslant 0$ and $\alpha_F, \alpha_B \geqslant 1$. Note that with this choice of potential, the contact forces effectively reduce to the Hunt and Crossley damped collision model [16].

This model incorporates the dynamics of the colliding finger and bow. If their masses are respectively m_F and m_B, their vertical positions obey the equations:

$$m_F \ddot{w}_F = f_F + f_{\text{ext},F} \qquad m_B \ddot{w}_B = f_B + f_{\text{ext},B} \tag{5}$$

with $f_{\text{ext},F,B}(t)$ any external forces applied on the finger or bow. These terms will later be useful when the player's input on the bow and finger force is introduced.

2.2.2 Contact force density for the neck

The neck is modelled as a rigid barrier at a distance $\varepsilon(x)$ under the string, with no damping. The contact force density between the string and the neck can therefore be written as:

$$\mathcal{F}_N = \frac{\partial \Phi_N}{\partial t} \Big/ \frac{\partial \Delta_N}{\partial t} \qquad \Phi_N = \frac{K_N}{\alpha_N + 1} (\Delta_N)_+^{\alpha_N + 1} \tag{6}$$

with $\Delta_N(x,t)$ the penetration, given as:

$$\Delta_N = \varepsilon - w \tag{7}$$

If K_N is a large enough number, the interaction tends towards a perfectly rigid collision.

2.2.3 Energy analysis for the vertical polarisation

As the two polarisations are not intrinsically coupled, the energy analysis can be separately performed on each of the equations from (1). For the vertical polarisation, let us multiply (1a) by $\frac{\partial w}{\partial t}$ and integrate the equation over S, which yields, after replacing the force terms by their respective expressions:

$$\dot{H}_{w,s} + \dot{H}_N + \dot{H}_F + \dot{H}_B = -\mathcal{Q}_w + \mathcal{P}_w \tag{8}$$

where

$$H_{w,s} = \int_S \frac{\rho}{2} \left(\frac{\partial w}{\partial t} \right)^2 + \frac{T}{2} \left(\frac{\partial w}{\partial x} \right)^2 + \frac{B}{2} \left(\frac{\partial^2 w}{\partial x^2} \right)^2 dx \tag{9a}$$

$$H_N = \int_S \Phi_N \, dx \tag{9b}$$

$$H_F = \Phi_F + \frac{m_F}{2} \dot{w}_F^2 \tag{9c}$$

$$H_B = \Phi_B + \frac{m_B}{2} \dot{w}_B^2 \tag{9d}$$

$\mathcal{Q}_w \geqslant 0$ is the power lost through damping in the string, finger, and bow, that is:

$$\mathcal{Q}_w = \lambda_1 \rho \int_S \left(\frac{\partial w}{\partial t} \right)^2 dx + \lambda_2 \rho \int_S \left(\frac{\partial^2 w}{\partial t \partial x} \right)^2 dx + \dot{\Delta}_F^2 \Psi_F + \dot{\Delta}_B^2 \Psi_B \tag{10}$$

$\mathcal{P}_w$ is the power supplied or withdrawn through external excitation:

$$\mathcal{P}_w = \dot{w}_F f_{\text{ext},F} + \dot{w}_B f_{\text{ext},B} + f_F \int_S w \frac{\partial J_F}{\partial t} dx + f_B \int_S w \frac{\partial J_B}{\partial t} dx \tag{11}$$

The choice of boundary conditions (simply supported) leads to the vanishing of the boundary terms in the power balance. As, by construction, $\Phi(x,t) \geqslant 0$ and $\Psi(x,t) \geqslant 0$, in the absence of driving terms, the system is strictly dissipative.

2.3 Friction interaction in the horizontal polarisation

2.3.1 Friction curve model

The friction model used here is that of a tangential friction force induced by the normal forces exerted by the bow, finger and neck; these normal forces are indeed the nonlinear contact forces, that are independently given by equation (1a). With Coulomb friction, the general expression for a tangential force F_t arising from a normal force F_n is $F_t = \varphi F_n$, with φ a coefficient of friction.

A variation on the original Coulomb friction is used in this model, that makes use of a dynamic friction coefficient. It is a widespread practice, especially for bowed string models [17], to assume that φ solely depends on the relative velocity between the two rubbing objects. Improved models have been used to describe the bow-string interaction [18, 19]; for the purposes of this paper, let us restrict attention to a simpler case, defining a *friction curve* $\varphi(v_{\text{rel}}(x,t))$ of the form:

$$\varphi(v_{\text{rel}}) = \sqrt{2\sigma} v_{\text{rel}} e^{-\sigma v_{\text{rel}}^2 + 0.5} + \mu_D \frac{2}{\pi} \arctan \frac{v_{\text{rel}}}{0.02} \tag{12}$$

where $\sigma > 0$ is a free parameter, that can be different for each separate interaction. μ_D is the dynamic friction coefficient, that is the constant value friction takes for large enough relative velocities; it is usually evaluated, for a rosin coated violin bow, as $\mu_D = 0.3$ [19]. Figure 2 shows $\varphi(v_{\text{rel}})$ for different values of σ. This model is somewhat different from the common hyperbolic curve, but the continuity at $v_{\text{rel}} = 0$ simplifies the numerical implementation [20]. The relative velocities of the neck $v_{\text{rel},N}(x,t)$, finger $v_{\text{rel},F}(t)$ and bow $v_{\text{rel},B}(t)$ with respect to the string are:

$$v_{\text{rel},N} = \frac{\partial u}{\partial t} \quad v_{\text{rel},F} = \int_{\mathcal{S}} J_F \frac{\partial u}{\partial t} dx \quad v_{\text{rel},B} = \int_{\mathcal{S}} J_B \frac{\partial u}{\partial t} dx - v_B \tag{13}$$

where $v_B(t)$ is the transverse velocity of the bow. Note that the finger and neck are not moving in the horizontal plane, therefore their transverse velocity is simply zero, and their relative velocity with respect to the string is the string velocity itself.

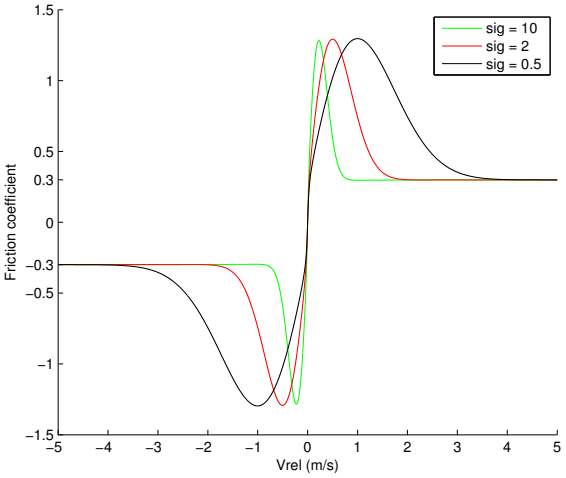

Figure 2: *Shape of the friction curve $\varphi(v_{\text{rel}})$ for different values of σ.*

2.3.2 Energy analysis for the horizontal polarisation

When multiplying equation (1b) by $\frac{\partial u}{\partial t}$ and integrating it over $\mathcal{S}$, a second power balance arises:

$$\dot{H}_{u,s} = -\mathcal{Q}_u + \mathcal{P}_u \tag{14}$$

where $H_{u,s}$ is analogous to $H_{w,s}$ defined in (9a):

$$H_{u,s} = \int_{\mathcal{S}} \left(\frac{\rho}{2} \left(\frac{\partial u}{\partial t} \right)^2 + \frac{T}{2} \left(\frac{\partial u}{\partial x} \right)^2 + \frac{B}{2} \left(\frac{\partial^2 u}{\partial x^2} \right)^2 \right) dx \tag{15}$$

$\mathcal{Q}_u \geqslant 0$ is the power dissipated through both the string internal damping and the friction between the objects and the string:

$$\mathcal{Q}_u = \lambda_1 \rho \int_{\mathcal{S}} \left(\frac{\partial u}{\partial t} \right)^2 dx + \lambda_2 \rho \int_{\mathcal{S}} \left(\frac{\partial^2 u}{\partial t \partial x} \right)^2 dx + \int_{\mathcal{S}} v_{\text{rel},N} \mathcal{F}_N \varphi_N + v_{\text{rel},F} \left(f_F \right)_+ \varphi_F + v_{\text{rel},B} \left(f_B \right)_+ \varphi_B \tag{16}$$

$\mathcal{P}_u$ is the power supplied to or withdrawn from the system in the horizontal polarisation, through the bow and finger motions:

$$\mathcal{P}_u = -v_B \left(f_B \right)_+ \varphi_B + \left(f_B \right)_+ \varphi_B \int_{\mathcal{S}} u \frac{\partial J_B}{\partial t} dx \tag{17}$$

$\mathcal{F}_N(x,t)$ is, by construction, positive for all $x \in \mathcal{S}$ and $t \in \mathbb{R}^+$. The system is thus strictly dissipative, in the absence of energy supply via the bow displacement, if the friction curve holds:

$$v_{\text{rel}} \varphi(v_{\text{rel}}) \geqslant 0 \tag{18}$$

3 Numerical implementation

A two-polarisation, one-dimensional finite difference scheme is designed for this model. Time is sampled at the audio rate of 44.1 kHz, and the domain $\mathcal{S}$ is discretised into a collection of $N+1$ equally spaced grid points $\mathcal{D} = \{0; 1; \ldots; N\}$. As the PDEs are second order in time, the state of the system at a given time step can be computed from at least the two previous samples. An energy-conserving finite difference scheme for a lumped contact problem has recently been established [21], that we can efficiently incorporate in this model. The contact force and tangential friction terms require the solution of two nonlinear systems at every time step, achieved with the Newton-Raphson algorithm (see [22] for its application to a similar contact problem). The output is obtained by successive iterations of this process; the data is read out as close to the bridge end as the model allows, in the horizontal polarisation, by a third order Lagrange interpolation between grid points. Convolution with a violin body impulse response gives rise to highly detailed and realistic synthetic sound.

3.1 Helmholtz motion

The simulation of the whole system allows for the full string displacement to be monitored in both polarisations, at any time. Typical Helmholtz motion was achieved with $f_{\text{ext},B} = 0.2$ N and $v_B = 0.3$ m/s in steady state, with the bow positioned at $x_B = 0.9L$ (hence a relative bow-bridge distance $\beta = 0.1$. The travelling of the Helmholtz corner can be observed in figure 3, with classic stick/slip cycles.

The waveform and relative velocity profile are consistent with previous experimental findings [23], as shown in figure 4.

The two polarisations can be observed at once by plotting the string displacement in a 3-dimensional space such as the one introduced in Figure 1. Figure 5 shows the string displacement at 3 instants withing a stick-slip cycle, while stopped by a finger pressing against the neck at three quarters of its length.

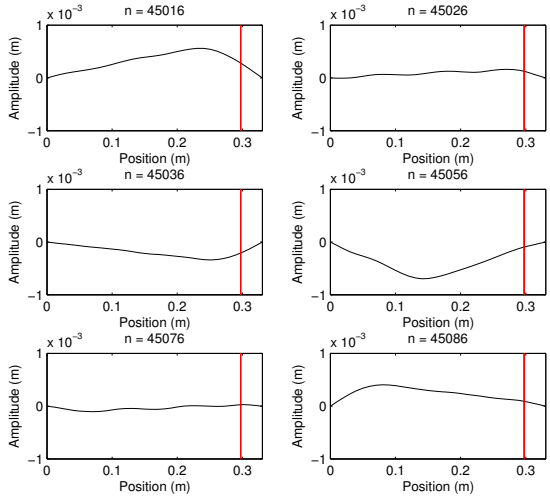

Figure 3: *Evolution of the string motion in the horizontal polarisation during one stick-slip cycle. The bow is represented by the vertical red line, moving upwards.*

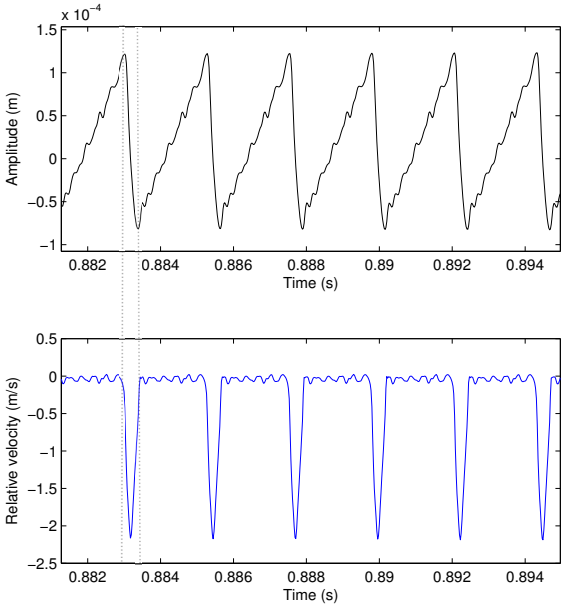

Figure 4: *Output waveform at the bridge end of the string in steady state, in the horizontal polarisation, and associated relative velocity profile.*

3.2 Gesture reproduction

Bowed string gestures are executed by coordinating a number of almost independent parameters, some of which are available for full dynamic control in this model. It is therefore possible to reproduce a variety of patterns found in bowed string performance, with the help of carefully coordinated input time series [13, 15]. Crescendi and diminuendi were achieved with linear variations of the bow velocity. A vibrato sound was synthesised with a simple sinusoidal variation of the finger position while the string was fretted; a linear variation gives rise to a glissando. The mass compliance of the bow also permits to simulate bouncing bow strokes, such as spiccato. A slightly varying bow-bridge distance allows for more realistic nuances in the synthetic sound; a more drastic drift towards the bridge end of the string, combined with an increase in bowing force, leads to a sharper sound, with increased high frequency content.

4 Conclusion

A two-polarisation physical model of a bowed string was designed, with nonlinear contact interactions in the vertical polarisation, and nonlinear friction forces in the horizontal polarisation. Energy dissipation was demonstrated in the absence of external excitation. A finite difference scheme was then established, based on the initial set of partial differential equations, and implemented to simulate the system. The resulting output agrees with previous experimental observations, as Helmholtz motion is obtained under the right bowing conditions. Such a numerical model requires a number of coordinated inputs, such as the bow velocity, bowing pressure, bow-bridge distance, finger position and force, which are easily and dynamically controlled over the length of the simulation. One can therefore achieve high quality sound synthesis, with a great level of realism and a wide range of reproducible gestures, whether it be bowing strokes (e.g., spiccato, détaché, crescendo…) or finger gestures (e.g., vibrato, glissando, etc.).

Full description and improvements on the finite difference scheme are left to a future publication, with the possible inclusion of finite width bow and finger. It is not difficult to imagine the coupling of a string with a bridge via a similar contact model, as a further step towards a full instrument physical model. The exploration of the bowing parameters space for this model is also yet to be fully achieved; the reproduction of Schelleng [24] and Guettler [25] diagrams would be one way to study the playability of the numerical model.

Sound examples obtained with the simulation are available on `http://www.ness-music.eu/target-systems/more/bowed-string-instruments`.

5 Acknowledgements

This work was supported by the European Research Council, under grant StG-2011-279068-NESS, and by the Edinburgh College of Art.

References

[1] L. Hiller and P. Ruiz, “Synthesizing musical sounds by solving the wave equation for vibrating objects: Part 2,” *J. Audio Eng. Soc*, vol. 19, no. 7, pp. 542–551, 1971.

[2] R. Bacon and J. Bowsher, “A discrete model of a struck string,” *Acta Acustica united with Acustica*, vol. 41, no. 1, pp. 21–27, 1978.

[3] K. Karplus and A. Strong, “Digital synthesis of plucked-string and drum timbres,” *Computer Music Journal*, vol. 7, no. 2, pp. 43–55, 1983.

[4] J. O. Smith III, “A new approach to digital reverberation using closed waveguide networks,” in *Proceedings of*

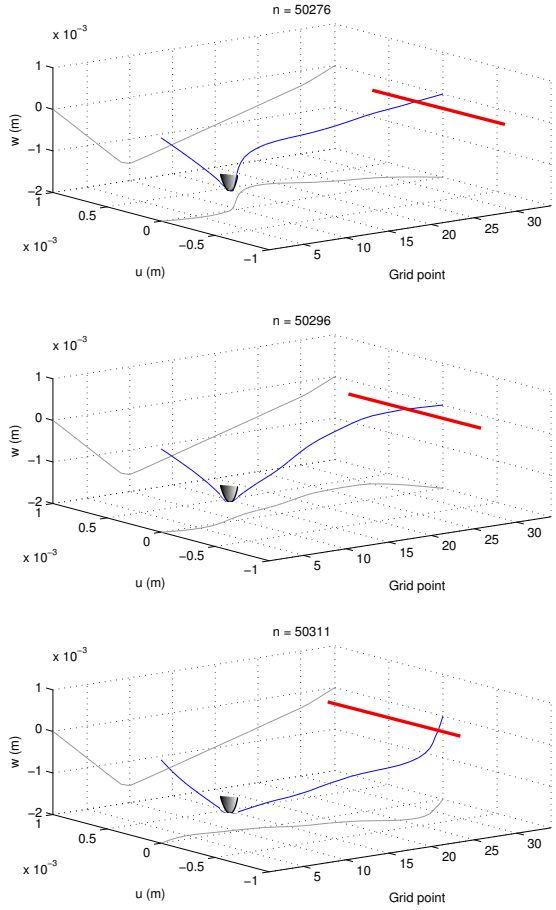

Figure 5: *3-dimensional plot of the two polarisations of the moving simulated string. The string slips against the bow between the last two frames. The bow is materialised by the red line. Note that the string is captured between the finger and the neck; for clarity, the latter was not drawn on this plot. The projections of the string displacement in the vertical and horizontal polarisations are drawn in light grey.*

the 1985 International Computer Music Conference, 1985, pp. 47–53.

[5] M. Karjalainen, V. Välimäki, and T. Tolonen, "Plucked-string models: From the Karplus-Strong algorithm to digital waveguides and beyond," *Computer Music Journal*, pp. 17–32, 1998.

[6] D. Kartofelev, A. Stulov, H.-M. Lehtonen, and V. Välimäki, "Modeling a vibrating string terminated against a bridge with arbitrary geometry," 2013.

[7] J. C. Strikwerda, *Finite difference schemes and partial differential equations*. Siam, 2004.

[8] D. Young and S. Serafin, "Playability evaluation of a virtual bowed string instrument," in *Proceedings of the 2003 conference on New interfaces for musical expression*. National University of Singapore, 2003, pp. 104–108.

[9] S. Serafin and D. Young, "Bowed string physical model validation through use of a bow controller and examination of bow strokes," *Proc. Stockholm Musical Acoustics Meeting (SMAC)*, 2003.

[10] C. Poepel, "Synthesized strings for string players," in *Proceedings of the 2004 conference on New interfaces for musical expression*. National University of Singapore, 2004, pp. 150–153.

[11] A. Askenfelt, "Measurement of bow motion and bow force in violin playing," *The Journal of the Acoustical Society of America*, vol. 80, no. 4, pp. 1007–1015, 1986.

[12] ——, "Measurement of the bowing parameters in violin playing. II: Bow-bridge distance, dynamic range, and limits of bow force," *The Journal of the Acoustical Society of America*, vol. 86, no. 2, pp. 503–516, 1989.

[13] M. Demoucron, "On the control of virtual violins-physical modelling and control of bowed string instruments," Ph.D. dissertation, Université Pierre et Marie Curie-Paris VI, 2008.

[14] E. Maestre-Gomez *et al.*, "Modeling instrumental gesture: An analysis/synthesis framework for violin bowing," Ph.D. dissertation, Univ. Pompeu Fabra, Barcelona, 2009.

[15] E. Maestre, "Analysis/synthesis of bowing control applied to violin sound rendering via physical models," in *Proceedings of Meetings on Acoustics*, vol. 19, no. 1. Acoustical Society of America, 2013, p. 035016.

[16] K. Hunt and F. Crossley, "Coefficient of restitution interpreted as damping in vibroimpact," *Journal of Applied Mechanics*, vol. 42, no. 2, pp. 440–445, 1975.

[17] M. McIntyre and J. Woodhouse, "On the fundamentals of bowed-string dynamics," *Acta Acustica united with Acustica*, vol. 43, no. 2, pp. 93–108, 1979.

[18] J. H. Smith and J. Woodhouse, "The tribology of rosin," *Journal of the Mechanics and Physics of Solids*, vol. 48, no. 8, pp. 1633–1681, 2000.

[19] S. Serafin, J. O. Smith III, and J. Woodhouse, "An investigation of the impact of torsion waves and friction characteristics on the playability of virtual bowed strings," in *Applications of Signal Processing to Audio and Acoustics*. IEEE, 1999, pp. 87–90.

[20] S. Bilbao, *Numerical Sound Synthesis: Finite Difference Schemes and Simulation in Musical Acoustics*. Wiley Publishing, 2009.

[21] V. Chatziioannou and M. van Walstijn, "An energy conserving finite difference scheme for simulation of collisions," 2013.

[22] S. Bilbao, A. Torin, and V. Chatziioannou, "Numerical modeling of collisions in musical instruments," (in preparation for Forum Acusticum 2014).

[23] J. Woodhouse and P. Galluzzo, "The bowed string as we know it today," *Acta Acustica united with Acustica*, vol. 90, no. 4, pp. 579–589, 2004.

[24] J. C. Schelleng, "The bowed string and the player," *The Journal of the Acoustical Society of America*, vol. 53, no. 1, pp. 26–41, 2005.

[25] K. Guettler, "On the creation of the Helmholtz motion in bowed strings," *Acta Acustica united with Acustica*, vol. 88, no. 6, pp. 970–985, 2002.